The PAMELA Experiment: Preliminary Results after Two Years of Data Taking

E. Mocchiutti[1], O. Adriani[4,15], G. C. Barbarino[5,16], G. A. Bazilevskaya[12], R. Bellotti[6,17], M. Boezio[1]
E. A. Bogomolov[9], L. Bonechi[4,15], M. Bongi[4], V. Bonvicini[1], S. Bottai[4], A. Bruno[6,17]
F. Cafagna[6], D. Campana[5], R. Carbone[5,14], P. Carlson[8], M. Casolino[2], G. Castellini[3], M. P. De Pascale[2,14]
G. De Rosa[5], N. De Simone[2,14], V. Di Felice[2,14], D. Fedele[4,15], A. M. Galper[11], L. Grishantseva[11], P. Hofverberg[8]
G. Jerse[1,13], S. V. Koldashov[11], S. Y. Krutkov[11], A. N. Kvashnin[12], A. Leonov[11], O. Maksumov[12], V. Malvezzi[2]
L. Marcelli[2], W. Menn[10], V. V. Mikhailov[11], N. N. Nikonov[9], S. Orsi[8,2], G. Osteria[6], P. Papini[4], M. Pearce[8]
P. Picozza[2,14], M. Ricci[7], S. B. Ricciarini[1]4, M. Runtso[11], M. Simon[10], R. Sparvoli[2,14], P. Spillantini[2,15]
Y. I. Stozhkov[12], E. Taddei[4,15], A. Vacchi[1], E. Vannuccini[4], G. Vasilyev
footnotemark[9], S. A. Voronov[11], Y. T. Yurkin[11]
G. Zampa[1], N. Zampa[1], V. G. Zverev[11]

***Abstract*— PAMELA is a satellite–borne experiment designed to study charged particles in the cosmic radiation. The primary scientific goal is the study of the antimatter component of the cosmic–rays over the largest energy range ever achieved (antiprotons, 80 MeV – 100's GeV; and positrons, 50 MeV – 270 GeV) in order to search for evidence of dark matter particle annihilations. PAMELA is also searching for primordial antinuclei with unprecedent sensitivity, and its precise measurements of the antiparticle energy spectrum together with its precision studies of light nuclei and their isotopes are used to test cosmic–ray propagation models. Moreover, PAMELA is investigating low energy particles in the cosmic radiation which permit to study solar physics and solar modulation during the 24th solar minimum. Finally, the reconstruction of the cosmic ray electron energy spectrum up to several TeV allows a possible contribution from local sources to be studied. PAMELA is housed on–board the Russian Resurs–DK1 satellite, which was launched on June 15^{th} 2006 in an elliptical (350–610 km altitude) orbit with an inclination of 70 degrees. The status of the PAMELA experiment is reviewed, and scientific results after two years in flight are presented.**

[1]INFN, Sezione di Trieste, I-34012 Trieste, Italy, Emiliano.Mocchiutti@ts.infn.it
[13]Physics Department of University of Trieste, I-34127 Trieste, Italy
[2]INFN, Sezione di Roma "Tor Vergata", I-00133 Rome, Italy
[14]Physics Department of University of Rome "Tor Vergata", I-00133 Rome, Italy
[3]IFAC, I-50019 Sesto Fiorentino, Florence, Italy
[4]INFN, Sezione di Florence, I-50019 Sesto Fiorentino, Florence, Italy
[15]Physics Department of University of Florence, I-50019 Sesto Fiorentino, Florence, Italy
[5]INFN, Sezione di Naples, I-80126 Naples, Italy
[16]Physics Department of University of Naples "Federico II", I-80126 Naples, Italy
[6]INFN, Sezione di Bari, I-70126 Bari, Italy
[17]Physics Department of University of Bari, I-70126 Bari, Italy
[7]INFN, Laboratori Nazionali di Frascati, Via Enrico Fermi 40, I-00044 Frascati, Italy
[8]KTH, Department of Physics, AlbaNova University Centre, SE-10691 Stockholm, Sweden
[9]Ioffe Physical Technical Institute, RU-194021 St. Petersburg, Russia
[10]Physics Department of Universität Siegen, D-57068 Siegen, Germany
[11]Moscow Engineering and Physics Institute, RU-11540 Moscow, Russia
[12]Lebedev Physical Institute, RU-119991 Moscow, Russia

I. INTRODUCTION

The WiZard collaboration is a scientific program devoted to the study of cosmic rays through balloon and satellite borne devices. The main stream of physics goals our collaboration is devoted to include the precise determination of the antiproton [1] and positron [2] spectrum, the search of antimatter, the measurement of low energy trapped, and solar cosmic rays (NINA-1 [3] and NINA-2 [4] satellite experiments). Other research on board Mir and International Space Station has involved the measurement of the radiation environment, the nuclear abundances, and the investigation of the Light Flash phenomenon with the Sileye experiments [5], [6]. At present PAMELA is the largest and most complex device built by our collaboration. In this work we describe the scientific objectives, the detector and the first preliminary results of PAMELA after two years of data taking.

II. INSTRUMENT AND SCIENCE

PAMELA aims to measure in great detail the cosmic ray component at 1 AU (Astronomical Unit). Its 70 degrees, 350–610 km quasi–polar elliptical orbit makes it particularly suited to study items of galactic, heliospheric, and trapped nature. PAMELA has been mainly conceived to perform high–precision spectral measurement of antiprotons and positrons and to search for antinuclei, over a wide energy range. Besides the primary objective to study cosmic antimatter, the instrument setup and the flight characteristics allow many additional scientific goals to be pursued. Due to the high–identification capabilities of the instrument light nuclei and their isotopes, as well, at least up to Z=8, can be identified. This provides complementary data, besides antimatter abundances, to test models for the origin and propagation of galactic cosmic rays. In addition, the low–cutoff orbit and long–duration mission

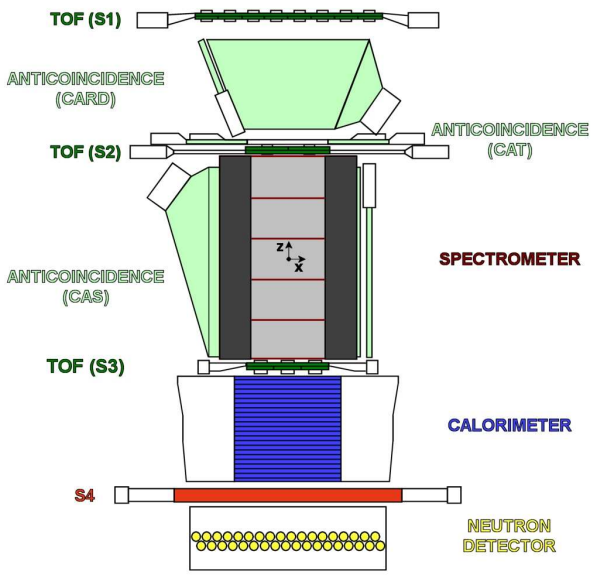

Fig. 1. A schematic view of the PAMELA apparatus. The instruments is ∼1.3 m tall and has a mass of 470 kg. The average power consumption is 355 W. Magnetic field lines inside the spectrometer are oriented parallel to the y direction.

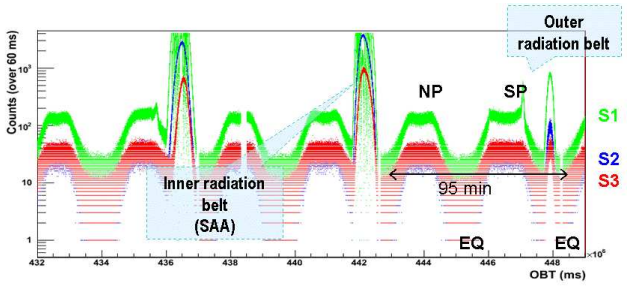

Fig. 2. Counting rates of S1 (green), S2 (blue) and S3 (red) as function of the On Board Time (OBT). During these three orbits the South Atlantic Anomaly (SAA) is crossed twice.

permits to detect low–energy particles (down to 50 MeV) and to follow long–term time variations of the radiation intensity and transient phenomena. This allows to extend the measurements down to the solar–influence energy region, providing unprecedented data about spectra and composition of solar energetic particles and allowing to study solar modulation of galactic cosmic rays over the minimum between solar cycles 23 and 24. Finally, the satellite orbit spans over a significantly large region of the Earth magnetosphere, making possible to study its effect on the incoming radiation. A more detailed overview of the PAMELA scientific goal can be found in [7].

The instrument is installed inside a pressurized container (2 mm aluminum window) attached to the Russian Resurs–DK1 Earth–observation satellite that was launched into Earth orbit by a Soyuz–U rocket on June 15^{th} 2006 from the Baikonur cosmodrome in Kazakhstan. The mission is foreseen to last till at least December 2009.

The PAMELA apparatus comprises the following subdetectors, arranged as shown in Figure 1 (from top to bottom): a time–of–flight system (TOF – S1, S2, S3); a magnetic spectrometer; an anticoincidence system (CARD, CAT, CAS); an electromagnetic imaging calorimeter; a shower tail catcher scintillator (S4) and a neutron detector. Planes of plastic scintillator mounted above and below the spectrometer form the TOF system, which also provide a fast signal for triggering the data acquisition. The timing resolution of the TOF system allows albedo–particle identification and mass discrimination below 1 GeV/c. The central part of the PAMELA apparatus is the magnetic spectrometer consisting of a 0.43 T permanent magnet and a silicon tracking system, composed of 6 planes of double–sided microstrip sensors. The spectrometer measures the rigidity (momentum over charge) of charged particles and the sign of the electric charge through their deflection (inverse of rigidity) in the magnetic field. Ionization losses are measured in the TOF scintillator planes, the silicon planes of the tracking system and the first silicon plane of the calorimeter allowing the absolute charge of traversing particles to be determined. The acceptance of the spectrometer, which also defines the overall acceptance of the PAMELA experiment, is 21.5 cm^2sr and the spatial resolution of the tracking system is better than 4 μm up to a zenith angle of 10°, corresponding to a maximum detectable rigidity (MDR) exceeding 1 TV. The spectrometer is surrounded by a plastic scintillator veto shield, aiming to identify false triggers and multiparticle events generated by secondary particles produced in the apparatus. Additional information to reject multiparticle events comes from the segmentation of the TOF planes in adjacent paddles and from the tracking system. An electromagnetic calorimeter (16.3 X_0, 0.6 λ_0) mounted below the spectrometer measures the energy of incident electrons and allows topological discrimination between electromagnetic and hadronic showers, or non–interacting particles. A plastic scintillator system mounted beneath the calorimeter aids in the identification of high–energy electrons and is followed by a neutron detection system for the selection of high–energy electrons which shower in the calorimeter but do not necessarily pass through the spectrometer. For this purpose, the calorimeter can also operate in self–trigger mode to perform an independent measurement of the lepton component up to 2 TV. More technical details about the entire PAMELA instrument and launch preparations can be found in [8].

III. ORBITAL ENVIRONMENT

PAMELA was first switched on June 21^{st} 2006 and it has been collecting data continuosly since July 11^{th} 2006. To date about 650 days of data have been analyzed, corresponding to more than one billion recorded triggers and about 12 TB data.

A typical behaviour of the acquisition of the device is shown in figure 2. The three colours represent the the counting rate of the three planes of the time of flight and correspond to particles of increasing energy: S1 is triggered by 36 MeV protons and 3.5 MeV electrons, S2 requires protons and electrons of 63 and 9.5 MeV, respectively, and S3 requires protons and electrons of 80 and 50 MeV (lower energy particles may penetrate the

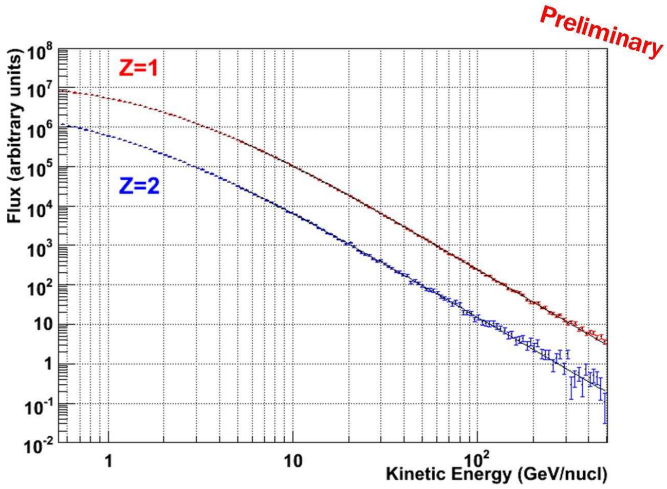

Fig. 3. Proton and helium nuclei spectra in arbitraty units.

detector from the sides and increase the trigger rate). The passages in the South Atlantic Anomaly (SAA) saturate several times the ADC counting rate of the S1 scintillator but not the other two scintillators. This is consistent with the power law spectrum of trapped particles in the SAA and the geometrical ratio between the two scintillators. Outside the SAA it is possible to see the increase of particle rate at the geomagnetic poles (North Pole, NP, and South Pole, SP) due to the lower geomagnetic cutoff. The highest rates are found when the satellite crosses the trapped components of the radiation belts (Van Allen Belts). The acquisition trigger rate depends on the used scintillator planes used to trigger an event (trigger configuration). The configuration that was found to maximize the collected number of good cosmic-ray events makes use of S1, S2 and S3 in the low-radiation environment and of S2 and S3 in the high radiation environment (magnetic poles and SAA). Since only S1 is affected by SSA radiation, this plane has been excluded from the trigger condition for high-radiation environment. Switch between the two acquisition modes is performed when the counting rate of S1 exceeds a given threshold. The overall average trigger rate is of about 25 Hz.

IV. PRELIMINARY RESULTS

A. Galactic cosmic rays

The most common particles in the cosmic radiation, protons and helium nuclei, are detected by PAMELA with very high statistics over a wide energy range. This allows to perform a precise measurements of their spectral shape and makes possible to study time variations and transient phenomena. The measurement of the spectra of primary cosmic rays have deep astrophysical implications and the importance of knowing the absolute values of the fluxes is essential to perform, for example, atmospheric neutrino observations. Figure 3 shows the preliminar protons (Z=1) and helium nuclei (Z=2) fluxes measured by PAMELA as function of the particle kinetic energy per nucleon. Only few months of data were used to produce this figure.

B. Solar modulation of GCR

Launch of PAMELA occurred during the 23^{rd} solar minimum. In this period it is be possible to observe solar modulation of galactic cosmic rays due to varying solar activity. A long term measurement of the proton, electron, and nuclear flux at 1 AU provides information on propagation phenomena occurring in the heliosphere. As already mentioned, the possibility to identify the antiparticle spectra allows to study also charge dependent solar modulation effects. Figure 4 shows the proton flux as measured by PAMELA in three different months in 2006, 2007 and 2008. To a decreasing solar activity corresponds an increasing flux of galactic cosmic rays. This effect is in agreement with the increase of neutron monitor fluxes [9].

C. Primary and re-entrant albedo measurements

Albedo particles are secondary particles produced by cosmic-rays interacting with the Earth's atmosphere that are scattered upward. When these particles lack sufficient energy to leave the Earth's magnetic field they re-enter the atmosphere in the opposite hemisphere but at a similar magnetic latitude and they are called re-entrant albedo particles. The measurement of the composition and spectra of the secondary cosmic rays particles provides a tool for the fine tuning of models used in air shower simulation programs. The importance of the programs for simulation of atmospheric showers has been emphasized in connection to the atmospheric neutrino observations performed by underground experiments. In fact a correct interpretation of these measurements depends on the accuracy of the predictions to which they are compared. Due to its orbit PAMELA is able to provide a world map of the primary and re-entrant albedo particles, allowing to discern fine details in the spectra especially in the sub-cutoff region.

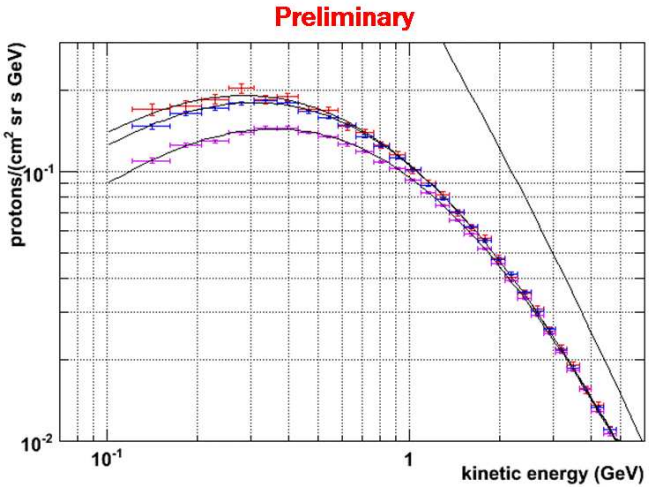

Fig. 4. Proton flux measured by PAMELA in July 2006 (violet), August 2007 (blue) and February 2008 (red). Solid line is a fit of the interstellar spectrum at energies greater than 20 GeV.

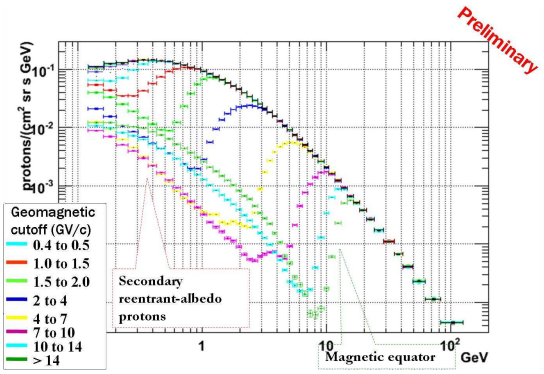

Fig. 5. Primary and re-entrant albedo proton spectra as function of the geomagnetic cutoff.

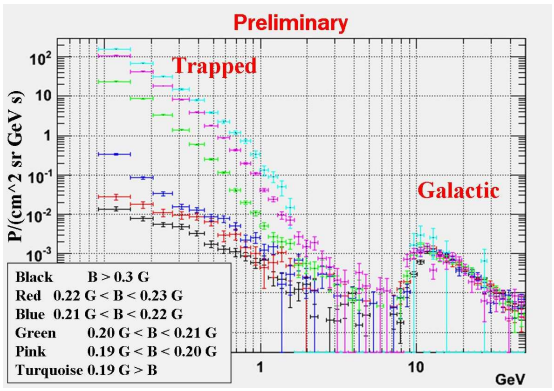

Fig. 6. Differential proton energy spectra of PAMELA in different regions of the South Atlantic Anomaly. The chosen regions are selected according to decreasing intensity of the magnetic field as described in the legenda.

Figure 5 shows the proton spectra at different geomagnetic latitudes. For each spectra is clearly visible the position of the geomagnetic cutoff and the secondary proton component due to re-entrant albedo particles. It is also possible to observe structures in the spectra, for example violet data between 3 and 5 GeV, that are also reproduced by simulations [10].

D. Trapped particles

The 70° orbit of the Resurs–DK1 satellite allows for continuous monitoring of the electron and proton belts. The high energy (>80 MeV) component of Van Allen Belts can be monitored in detail and it is possible to perform a detailed mapping of these regions by determining spectral and geometrical features [11]. Also the neutron component can be measured, although some care needs to be taken to estimate the background coming from proton interaction with the main body of the satellite. Figure 6 shows the differential proton energy spectra in different regions of the South Atlantic Anomaly. Data samples are selected according to the intensity of the magnetic field, lower the field the deeper inside the anomaly and the higher the proton flux. The flux of trapped protons can exceed the secondary particle flux in the same cutoff region outside the anomaly of about four orders of magnitude at low energy.

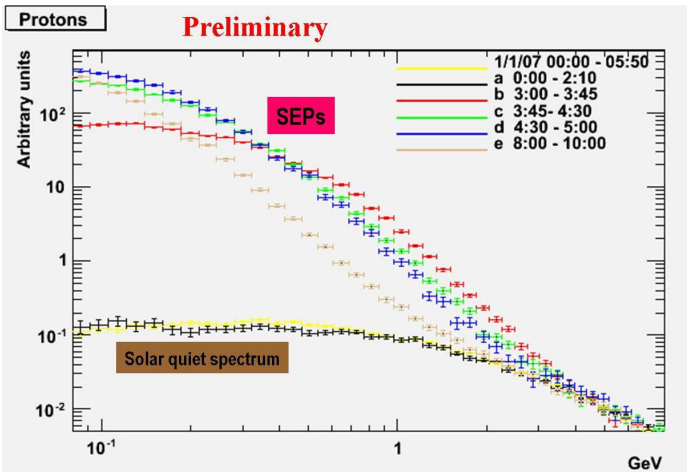

Fig. 7. Time variation of the proton flux during the December 13^{th} 2006 event.

E. Solar energetic particles

Due to the period of solar minimum few significant solar events with energy high enough to be detectable are expected. The observation of solar energetic particle (SEP) events with a magnetic spectrometer will allow several aspects of solar and heliospheric cosmic ray physics to be addressed for the first time.

Positrons are produced mainly in the decay of π^+ coming from nuclear reactions occurring at the flare site. Up to now, they have only been measured indirectly by remote sensing of the gamma ray annihilation line at 511 keV. Using the magnetic spectrometer of PAMELA it is possible to separately analyze the high energy tail of the electron and positron spectra at 1 AU obtaining information both on particle production and charge dependent propagation in the heliosphere in perturbed conditions of solar particle events.

PAMELA will is able to measure the spectrum of cosmic ray protons from 80 MeV up to almost 1 TeV and therefore is able to measure the solar component over a very wide energy range (where the upper limit will be limited by statistics). These measurements can be correlated with other instruments placed in different points of the Earth's magnetosphere to give information on the acceleration and propagation mechanisms of SEP events. Figure 7 shows, as example, the time variation of the the proton flux as consequence of the solar event of December 13^{th} 2006. Different colors represent the measured flux as function of the time. The solar quiet proton spectrum is shown as it was before December 13^{th} (black) and after (yellow) the December 13^{th} event. It is possible to notice that the high statistic allows to precisely measure the proton flux in very small time intervals and hence to study accurately the evolution of the solar event.

Furthermore PAMELA can also investigate the light nuclear component related to SEP events over a wide energy range. These measurements will help us to better understand the selective acceleration processes in the higher energy impulsive events [12]. Finally the high inclination of the orbit of the

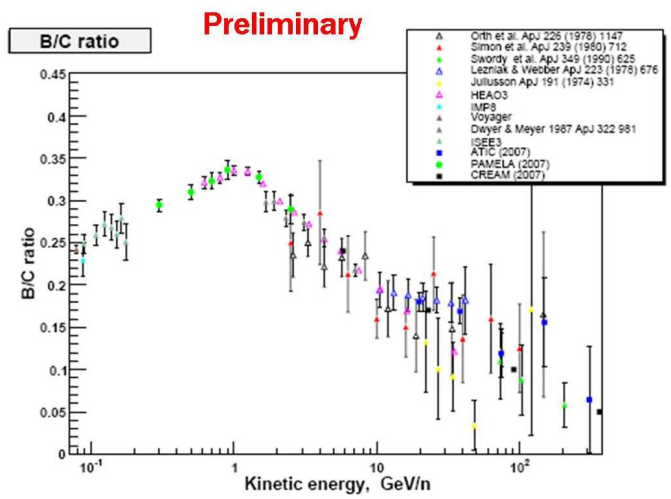

Fig. 8. PAMELA Boron to Carbon ratio compared to previous measurements.

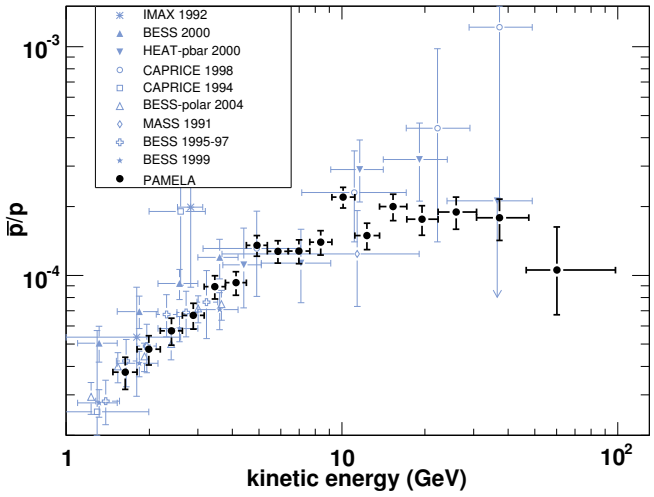

Fig. 9. The antiproton-to-proton flux ratio obtained by PAMELA [22] compared with contemporary measurements [23], [24], [25], [26], [27], [28], [29].

Resurs-DK1 satellite allows PAMELA to study [13], [14] the variations of cosmic ray geomagnetic cutoff due to the interaction of the SEP events with the geomagnetic field.

F. Nuclei

Also light nuclei (up to Oxygen) are detectable with the scintillator system. In this way it is possible to study with high statistics the secondary/primary cosmic ray nuclear and isotopic abundances such as B/C, Be/C, Li/C, and ^{3}He/^{4}He. These measurements can constrain existing production and propagation models in the galaxy, providing detailed information on the galactic structure and the various mechanisms involved. Figure 8 shows very preliminary B/C ratio as function of kinetic energy per nucleon. PAMELA results (green circles) are in very good agreement with previous measurements.

G. Antiparticle measurements

The main task of PAMELA is to identify antimatter components against the most abundant cosmic–ray components. At high energy, main sources of background in the antimatter samples come from spillover (protons in the antiproton sample and electrons in the positron sample) and from like–charged particles (electrons in the antiproton sample and protons in the positron sample). Spillover background comes from the wrong determination of the charge sign due to measured deflection uncertainty; its extent is related to the spectrometer performances and its effect is to set a limit to the maximum rigidity up to which the measurement can be extended. The like–charged particle background is related to the capability of the instrument to perform electron–hadron separation.

Electrons in the antiproton sample can be easily rejected by applying conditions on the calorimeter shower topology, while the main source of background comes from spillover protons. In order to reduce the spillover background and accurately measure antiprotons up to the highest possible energy, strict selection criteria were imposed on the quality of the fitted track and the absolute value of the measured deflection was required to be 10 times larger than its estimated error. To measure the antiproton–to–proton flux ratio the different calorimeter selection efficiencies for antiprotons and protons were estimated. The difference is due to the momentum dependent interaction cross sections for the two particles. These efficiencies were studied using both simulated antiprotons and protons, and proton samples selected from the flight data. In this way, it was possible to normalize the simulated proton, and therefore the antiproton, selection efficiency. The selected proton and antiproton samples could be contaminated by pions produced by cosmic-ray interactions with the PAMELA payload. This contamination was studied using both simulated and flight data and was estimated to be less than 5% above 2 GV decreasing at less than 1% above 5 GV.

Figure 9 shows the antiproton–to–proton flux ratio measured by the PAMELA experiment [22] compared with other contemporary measurements. Only statistical error are shown since the systematic uncertainty is less than a few percent of the signal, which is significantly lower than the statistical uncertainty. The PAMELA data are in excellent agreement with recent data from other experiments, the antiproton–to–proton flux ratio increases smoothly with energy up to about 10 GeV and then levels off. The data follow the trend expected from secondary production calculations and our results are sufficiently precise to place tight constraints on secondary production calculations and contributions from exotic sources, e.g. dark matter particle annihilations.

Proton contamination in the positron sample can be reduced to a negligible amount using strong selection criteria on the topology of the shower inside the calorimeter and by requiring the match between the calorimeter detected energy and the tracker measured momentum. Using particle beam data collected at CERN we have previously shown [21] that a proton rejection power of 10^5 can be achieved up to 200 GeV/c

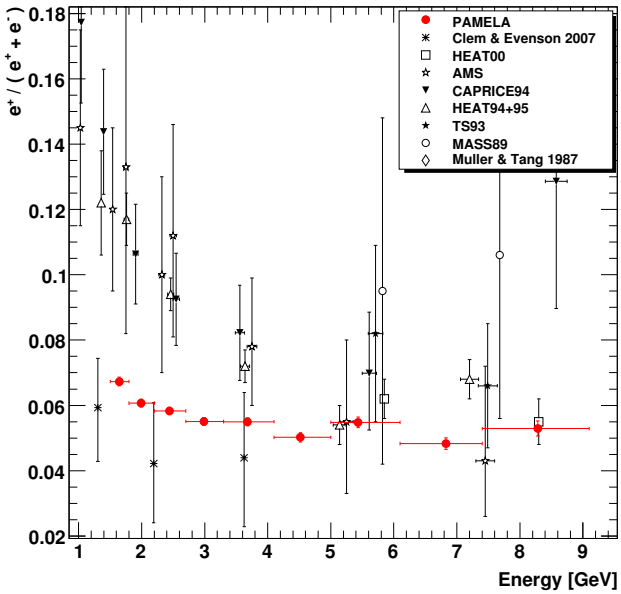

Fig. 10. The PAMELA positron fraction [30] compared to other experimental results[31], [32], [33], [34], [35], [36], [37], [38].

keeping an electron selection efficiency of 80%. A different approach has also been used to measure the high energy positron flux. This approach consist in keeping a very high selection efficiency and in quantifying the residual proton contamination [30]. Results are shown in figure 10, where PAMELA data are compared to other contemporary measurements. At low energy PAMELA data are lower than most of the other data and this can be interpreted as an observation of charge-sign dependent solar modulation effects. PAMELA data are in agreement with results from a balloon–borne experiment which flew in June 2006 [38] which observed a low positron fraction at low energies, but with large statistical uncertainties. At higher energies and below 10 GeV the PAMELA positron fraction is compatible with other measurements but does not confirm the structure between 6 and 10 GeV which was claimed previously by the HEAT experiment [39].

PAMELA is continuously taking data and the mission is planned to continue until at least December 2009. The increase in statistics will allow higher energies to be studied. An analysis for low energy antiprotons and positrons (down to 100 MeV) is in progress and will be the topic of future publications.

ACKNOWLEDGEMENTS

We would like to acknowledge contributions and support from: Italian Space Agency (ASI), Deutsches Zentrum für Luft– und Raumfahrt (DLR), The Swedish National Space Board, Swedish Research Council, Russian Space Agency (Roskosmos, RKA) and russian grants: RFBR grant 07-02-00992a and Rosobr grant 2.2.2.2.8248.

REFERENCES

[1] M. Boezio et al., Astrophys. J. 487, 415 (1997).
[2] M. Boezio et al., Astrophys. J. 532, 653 (2000).
[3] V. Bidoli et al., Astrophys. J. 132, 365 (2001).
[4] V. Bidoli et al., J. Geophys. Res. 108(A5), 1211 (2003).
[5] M. Casolino et al., Nature, 422 (2003).
[6] M. Casolino et al., Adv. Space Res. 37 (9), 1691 (2006).
[7] P. Picozza et al., in Proc. of 20^{th} ECRS, Lisbon – Portugal (2006).
[8] P. Picozza et al., Astrophys. J., 27, 296 (2007).
[9] Look for example http://neutronm.bartol.udel.edu/modplot.html .
[10] M. Honda, et al., Phys. Rev. D70/4, 043008 (2004).
[11] M. Casolino et al., in Proc. Int. Workshop on Adv. in Cosmic Ray Science, Waseda University, Shinjuku, Tokyo, Japan (2008).
[12] D. V. Reames, Space Sci. Rev. 90, 413 (1999).
[13] R. C. Ogliore, R.C. Mewaldt, R.A. Leske, et al., in Proc. of the 27th Int. Cosmic Ray Conf., Hamburg (2001).
[14] R. A. Leske, R. C. Mewaldt, E. C. Stone, T. T. von Rosenvinge, J. Geophys. Res. A 12, 30011 (2001).
[15] G. Jungman, M. Kamionkowski, and K. Griest, Phys. Rep. 267, 195 (1996).
[16] G. Bertone, D. Hooper, and J. Silk, Phys. Rep. 405, 279 (2005).
[17] S. Hawking, Nature 248, 30 (1974).
[18] P. Kiraly et al., Nature 293, 120 (1981).
[19] E. A. Bogomolov et al., in Proc. 16^{th} Int. Cosmic Ray Conf. (Kyoto), vol 1, p.330 (1979).
[20] R. L. Golden et al., Phys. Rev. Lett. 43, 1196 (1979).
[21] M. Boezio et al., Astropart. Phys. 26, 111 (2006).
[22] O. Adriani et al., submitted to Phys. Rev. Lett., astro-ph 0810.4994 (2008).
[23] M. Boezio et al., Astrophys. J. 561, 787 (2001).
[24] A. S. Beach et al., Phys. Rev. Lett. 87, 271101 (2001).
[25] M. Hof et al., Astrophys. J. Lett. 467, 33 (1996).
[26] J. Mitchell et al., Phys. Rev. Lett. 76, 3057 (1996).
[27] M. Boezio et al., Astrophys. J. 487, 415 (1997).
[28] Y. Asaoka et al., Phys. Rev. Lett. 88, 051101 (2002).
[29] T. Hams et al., in Proc. 30^{th} Int. Cosmic Ray Conf. (Merida) (2006).
[30] O. Adriani et al., submitted to Nature, astro-ph 0810.4995 (2008).
[31] H. Gast, J. Olzem, and S. Schael in Proc. XLI Rencontres de Moriond, Electroweak Interactions and Unified Theories, 421-428 (2006).
[32] D. Müller, and K. K. Tang, Astrophys. J. 312, 183-194 (1987).
[33] R. L. Golden et al., Astrophys. J. 436, 769-775 (1994).
[34] S. W. Barwick et al., Astrophys. J. 482, L191-194 (1997).
[35] M. Boezio et al., Astrophys. J. 532, 653-669 (2000).
[36] J. Alcaraz et al., Phys. Lett. B 484, 10-22 (2000).
[37] J. J. Beatty et al., Phys. Rev. Lett. 93, 241102-241105 (2004);
[38] J. Clem and P. Evenson, in Proc. 30th ICRC, Merida (2007).
[39] S. Coutu et al., Astropart. Phys. 11, 429 (1999).